ejpmr, 2022,9(12), 178-188

SJIF Impact Factor 6.222

EUROPEAN JOURNAL OF PHARMACEUTICAL AND MEDICAL RESEARCH

www.ejpmr.com

Review Article

ISSN 2394-3211

EJPMR

COLEUS AMBOINICUS LEAVES ASSISTED GREEN SYNTHESIS OF METAL AND METAL OXIDE NANOPARTICLES WITH DIFFERENT APPLICATIONS: A REVIEW

Navya Rao, Deepa Mudaliyar*, Vaibhav Parhad, Shriniwas Patil

Alard College of Pharmacy, Marunje, PCMC- 411 057, Pune.

***Corresponding Author: Deepa Mudaliyar**

Alard College of Pharmacy, Marunje, PCMC- 411 057, Pune.

Article Received on 05/10/2022 **Article Revised on 26/10/2022** **Article Accepted on 16/11/2022**

ABSTRACT

Several attempts have been made for green synthesis of nanoparticles of different metals and metal oxides, revealing the significance of plant extracts in reducing metal source to nanoparticles and applications in various scientific domains. The present article focus on applications of *Coleus amboinicus* leaves extract in fabrication of nanoparticles of various metals like silver, gold, zinc oxide, and copper oxide. *Coleus amboinicus* is evergreen, perennial shrub, belonging to family Lamiaceae (Labiatae). Its leaves are reported to contain several nonpolar phytochemicals like terpenes. In respective research attempts, these metallic and metal oxide nanoparticles were evaluated for one or more applications like anti-microbial activity. Use of *Coleus amboinicus* polar extract indicated involvement of its phytocompounds in reducing the source and stabilizing the nanoparticles. In conclusion, it could be noted that metal and metal oxide nanoparticles have better antimicrobial activity over leaves extract.

KEYWORDS: *Coleus/ Plectranthus amboinicus*, aqueous extract, nanoparticles, antimicrobial activity.

INTRODUCTION

Nanoparticles - a novel drug delivery system refers to an emerging field of pharmaceutical science as it overcomes the limitations of traditional drug delivery systems. As the name suggests, NPs lie in the range of 01-100nm. Copper, zinc, magnesium, gold, titanium, silver and alginate are some of the metals presently being used to synthesize nanoparticles.[1] Some of the frequently used methods to prepare NPs are 1) Dispersion of preformed polymers, 2) polymerization of monomers and 3) ionic gelation or coacervation of hydrophilic polymers.

The reason behind the current demand for the usage of metallic nanoparticles as it seems to control the particle size and surface properties along with the release of the therapeutically active constituents to achieve site-specific pharmacological action at an optimal rate and dose regimen.[2] The pharmacological and pharmacognostical studies revealed to have antimicrobial, antiviral, antioxidant, antiplasmodial, antifungal, anti-inflammatory, antibacterial, antidiabetic and antineoplastic activity.Some non-pharmacological applications include fluorescent biological labels, drug and gene delivery, bio-detection of pathogens, protein detection, DNA structure probing, tissue engineering, tumour destruction, separation and purification of biological molecules and cells, MRI contrast enhancement and phagokinetic studies.[3]

Coleus aromaticus/amboinicus (Fig.1) is a herb belonging to the botanical family Lamiaceae (Labiatae) and *Coleus* which is now referred to as the *Plectranthus* genus. It is an aromatic perennial large succulent herb with a height of 30-90 cm. It is present with a thick fleshy stem and distinctive-smelling leaves with much branching. The plant is found distributed throughout India. It is cultivated both in India and Malaysia. With its distinctive aroma, it has several culinary usages even in South America, the Philippines, Indonesia, Africa, India and South East Asia. It is also seen to have several culinary usages because of its strong flavour and aroma. It has been reported to be used as a food supplement and flavouring for drinks and no cases of toxic ingestion have been reported except for some skin allergy. As a folkloric medicinal plant, it was reported to be used in malarial fever, hepatopathy, renal and vesical calculi, cough, chronic asthma, hiccough, bronchitis, helminthiasis, colic, convulsions, and epilepsy.[4]

Morphology

In India, *Coleus* is considered as a popular drug and is commonly called oregano. *Coleus amboinicus* is a perennial highly fragrant herb aged 03 -10 years old. This can climb and reach about 01 m in height with simple but thick leaves with a light blade and opposite type of leaves arrangement. Broad oval or triangular shapes with cutting bases and acute apex are seen extensively. The leaf margin is crenate and the lower surface contains glandular hairs. The flowers of the plant

are seen to have a bell-shaped calyx, a pale purplish corolla which is almost 5 X longer than the calyx.[2]

Fig. 1: Coleus amboinicus.

Phytochemical constituents

Essential oils were one of the major parts of chemical constituents of *Coleus*. This was obtained by Yuan-Siao Chen et al in 2014 by performing hydro-distillation of the stem and leaves. The plant was found to contain53% monoterpene hydrocarbons and other 45% constituents of oxygenated monoterpenes, sesquiterpenes, and oxygenated sesquiterpenes,including1–3 carvacrol, b-caryophyllene, q-cymene, c-terpinene, a-bergamotene, a-caryophyllene, eudesma-4,1-diene, 4-terpineol, a-cubebene, and caryophyllene oxide.

Pharmacological uses:- The herb has a huge traditional history and is considered one of the most effective drugs. It wasconsidered to be used in the treatment of cephalgia, otalgia, anorexia, dyspepsia bloating, colic, diarrhoea, cholera, gums, seizures, asthma, cough and chronic bronchitis among others. Review on the pharmacological uses of *Coleus amboinicus*by Punet kumar et al in 2020 in which they reviewed the Antimicrobial activity, Antifungal activity, anti-inflammatory activity, antibacterial activity, skin care, antidiabetic activity, anxiolytic, anxiolytic activity, diuretic activity, wound healing activity, respiratory disorders, antiurolithiatic activity, analgesic activity, rheumatoid activity, antiplatelet aggregation activity, antibiofilm efficacy and in non-pharmacological uses it was also found to show culinary uses.[5]

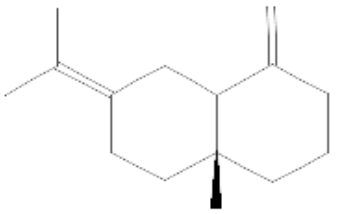

Eudesma-4,11-diene

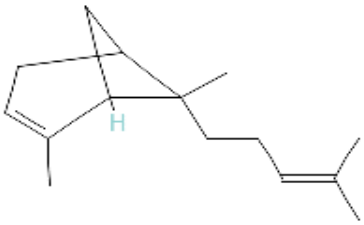

a-bergamotene

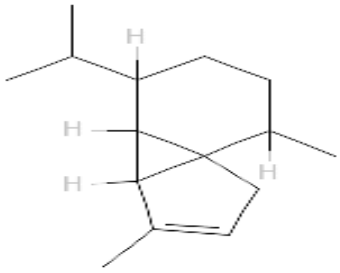

a-cubebene

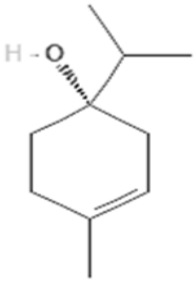

4-terpineol

Green synthesis of nanoparticles using *Coleus amboinicus* leaves

Reduced graphene oxide-supported palladium nanoparticles (RGO-PN)

Mallikarjuna et al. 2021 attempted green synthesis of reduced graphene oxide-supported palladium nanoparticles (RGO-PN) using an aqueous extract of *Coleus* leaves. They extracted 5 gm of powder of Coleus leaves in 50 ml of double distilled water and filtered them. Firstly, they prepared palladium-reduced graphene oxide (Pd-RGO) catalyst by sonicating 1 gm of graphene oxidein 70 mL distilled water for 30 min. Further, they synthesised reduced graphene oxide-supported palladium nanoparticles (RGO-PN) by treating (Pd-RGO) catalyst (in different concentrations, 50, 100 and 150 mg) with 10 ml *Coleus* leave extract in 70 ml of deionized water; and sonicated at room temperature for 8 hrs. Colour change observed in reaction mixture indicated the formation of reduced graphene oxide palladium nanoparticles (RGO-PN). The newly prepared nanoparticles were characterized by UV, XRD, SEM, TEM and XPS. UV visible absorption of synthesized RGO-PN of the 3 different concentrations showed strong and sharp absorption peaks in the range of 220-250 nm. The differences in the absorption spectra were seen due to the changes in the degree of bio-reduction of RGO-

supported palladium nanoparticles by the phenolic and flavonoid constituents of *Coleus amboinicus*. XRD patterns confirmed that the characteristic peaks of RGO-supported palladium nanoparticles correspond to the (111), (200), (220), (311), and (222) planes, thus confirming the pure cubic crystallite structure of green synthesized RGO-PN nanoparticles which were calculated from the Debye–Scherrer's formula. The SEM analysis depicted that the spherical-shaped green synthesized palladium nanoparticles were anchored with the reduced graphene oxide sheets whose size was found to be in the range of 20–40 nm. Whereas high resolution images were observed by TEM analysis with palladium nanoparticles also showing a spherical shape with a diameter of 20-30nm. Here, it must be noted that a high surface area to volume ratio was found insmaller particles which further influences the active sites for catalytic applications. The XPS analysis observed the Pd, C, and O elements in the survey scan of the green synthesized RGO-PN. The Palladium spectra also showed the presence of Pd^{2+}. The Carbon had an enlarged 1s spectra along with an enlarged spectra of Oxygen. The green synthesis of *Coleus amboinicus* showed that they served as an excellent catalytic reducing agent as it resulted in better reduction kinetics for 4-nitrophenol as they reduced the intensity to 294nm from 400nm in the span of 40 min. The biosynthesized leaf extract of *C.amboinicus* using Pd-RGO has effective antibacterial activity against *E.coli*. The green synthesized RGO (10 µg) nanoparticles showed a gradual increase in zone of inhibition at 2 mm (RGO), 4 mm (RGO-PN50), 12 mm (RGO-PN100), and 10 mm (RGO-PN150), respectively. Thus, proving that these *C.amboinicus* nanoparticles showed remarkable antibacterial activity against *E.coli*. Thus they concluded that the attempted RGO nanoparticles prepared using *Coleus amboinicus* could be used as a bio-reduction agent; along with having dual application in both environmental clean-up and pharmaceuticals.[6]

Ultrasonically driven palladium nanoparticles

Chinna bathula et al 2020 attempted ultrasonically driven green synthesis of Palladium NPs of *Coleus amboinicus*. They crushed and dried 05 g of the leaf powder and placed it in 30 mL of DDW. This was then placed in an ultrasonicator with the power of 40 kHz and 150 W for about 30 min. The extract was obtained on centrifugation and filtered for further process for the formation of Palladium NPs. The NPs were prepared by treating 0.01M $PdCl_2$ in 30mL DW under the same ultrasonic vibration as mentioned above and 03mL of the leaf extract. The reaction transitioned from brown to black colour suggesting a complete reduction. Characterization techniques like XRD, FTIR, TEM and SEM, UV, Catalytic Kinetics and Sizuki-Miyaura coupling reactions. The XRD diffraction plot confirmed patterns of Pure Cubic palladium NPs. The peaks had appeared at 41.3°, 46.7°, 54.5° and 80.8° which corresponded to the FCC structure with no impurity peaks. The TEM and SEM featured the morphological features of the Pd NP of *C.amboinicus*, with them defining a spherical and crystal morphology and size range of 16-23nm without agglomeration. The average particle size was approximately calculated to be 20nm. UV absorption spectra was done for the study of optical property. The absorption showed a wide pigment of 220-450 nm; while its precursor showed absorbance at 480 nm. The decrease was due to the reduction of Pd ions. FTIR analysis is preferred to confirm the presence of the various functional groups. The major bands corresponded to the formation of the metal NPs. The FG detected was from the N-H stretching and O-H vibration of amides and polyphenols in the leaf extract. Furthermore, a peak contributed to the carbon stretching vibration of OH moieties in carboxylic aid of the bio-reducing leaf extract. The catalytic reduction process was done to elucidate its kinetics. N-Nitro phenol and $NaBH_4$ were considered as standard and the bioinspired Pd NP of *C.amboinicus* was used as a catalyst. At a concentration of 0.5mL, the standard 400 nm value decreased over time and finally disappearing at 08 min with a peak of 294nm. By this, they obtained a short reduction time of 08 min implying that the prepared Pd NPs suspension could serve as an excellent catalytic reducing agent. The Suzuki-Miyaura coupling reactions were also determined with the ultrasonicator. They found out that the aryl halide had been completely converted into Bi-aryl compounds with excellent results when PEG-400 was used as a green solvent. This reaction of the NPs provided some advantages like increased efficiency, simplicity etc. They thus concluded that the suspension of green synthesis of *C.amboinicus* was useful and had quite a few applications.[7]

Silver nanoparticles

Vanaja et al 2012, undertook the research on the synthesis of silver nanoparticles of the leaf extract of *Coleus aromaticus* along with its antibacterial activity. The extract was prepared by washing with tween 20. About 10 g of leaves were cut and boiled at 60 °C for 5 min. For nanoparticles preparation, the above leaf extract was added to 90 mL of 01mM of $AgNO_3$ which was indicated by formation of brown colour. The thus prepared silver nanoparticles of *C. aromaticus* were characterized using UV along with XRD, SEM, EDAX and FTIR. They also screened the nanoparticles for their antibacterial activity. The UV–visible spectra of silver nanoparticles were measured at different time intervals ranging from 340-740nm and the strong SPR (surface plasmon resonance) bands were observed at 460 nm. This indicated the spherical shape while the broad peaks showed that the nanoparticles were monodispersed. The XRD peaks were observed at four distinct diffraction peaks which can be assigned to the plane of (1 1 1), (2 0 0), (2 2 0) and (3 1 1) respectively indicating the silver nanoparticles are FCC (face centred cubic) and crystalline in nature. The Debye–Scherrer's equation was used to estimate the mean size of the biosynthesized nanoparticles. The SEM image illustrated the spherical shape of particles and aggregated into larger particles. It

also showed the size of nanoparticles ranging from 40-50 nm. The formation of silver nanoparticles was confirmed by EDAX studies which showed strong signal of silver from 03 keV with weak signals from O. Weak signals of O due to X-ray emission from the various primary metabolites like carbohydrates/proteins/enzymes present within the leaves of *C.aromaticus*. The functional biomolecules associated with the FTIR were responsible for the reduction of silver ions. FTIR spectra shows the band that corresponds to the 'NH' group of amines. There was also the presence of a weak band which characterizes the O–H stretching of secondary alcohols. Some bands thus deduced the presence of C=O stretching of alcohols amide I band and nitro groups. C–N stretching vibrations of aromatic amines were also determined. The bacterial activity of the silver nanoparticles showed its toxicity on *B. subtilis* and *K. planticola* by disc diffusion method. The zone of inhibition was directly proportional to the increasing concentration of the nanoparticles (10-50 µL). At the highest concentration (50 µL) the nanoparticles inhibited the growth of Gram Negative bacteria around the disc of 11.00 ± 0.335 mm in diameter; while the zone of inhibition for the Gram Positive bacteria was found to be 12.33 ± 1.203 mm in diameter. They also briefly discussed the mechanism of action of the silver nanoparticles. They concluded by mentioning the various applications of *C.aromaticus* along with the benefits of using the above-preferred synthesis for the nanoparticles. In another study done by Vanaja et al 2013, they also researched the effects of the previously prepared silver nanoparticles on the effects of pH and temperature. The size of the synthesized NP was quite smaller (20-30nm) as compared to *Acalypha indica* (greater than 1000nm). The present investigation of the NP indicated that alkaline pH of 8.2 showed a narrow peak (460 nm) with a sharp peak. Temperature also showed effects on the particle aggregation as well as the absorption spectra in the UV. They also added a brief note of the chemical constituents and uses of *C. aromaticus*.[8]

Second attempt of synthesis of silver nanoparticles was made by Prajapati et al in 2020. They synthesise bio-inspired silver nanoparticles of *C. amboinicus* along with investigating its applications of spin-orbital interactions with light. Extract was prepared using 20g fresh and healthy leaves of *C.amboinicus* and chopped into small leaves upon rinsing with Double distilled water. Further, these were boiled using 100mL DDW for 05 min. Filter and cooled extract stored at 04°C for further synthesis. This filter acts as a reducing and stabilizing agent for nanoparticles synthesis. 05mL of the above solution was then added to 10^{-3}mM $AgNO_3$. The reaction is monitored through the UV-vis spectrum. The complex formation (the Ag^+ ions to the *Coleus* leaf extract) leads to a colour change from colourless to Yellow. Thus the bio-induced Silver Nanoparticles are collected and characterized. The particles were analysed by using spectroscopic techniques using UV and FTIR and also characterized the microscopic characters by studying TEM. For the dilution of the sample UV nanoparticles (0.4mL) was diluted with water (4mL) and analysed at room temperature. 03 different spectra was recorded at different time intervals. At t=0 there was no SPR peaks which indicated the absence of the nanoparticles. An increase in reaction duration t=30min they observed the SPR at 427nm and at t=60mins 435nm. This implied reduction of Ag^+ ions to form stable silver nanoparticles within an hour. This thus made this method one of the fastest bio-inspired methods. FTIR spectra was recorded for both fresh leaf extract and the synthesized nanoparticles. For the fresh extract 03 strong and 02 weak peaks were noticed to correspond C–Cl–, N–H bending, −C=C– aromatic and H bonded OH stretches, respectively while weak were at because of -C triple bond C stretching and S-H stretching thiol group. For the nanoparticles the peaks observed correspond to C=C bending, N–H bending, amine group and OH stretching alcohol group, respectively. TEM results indicated that most of the Ag NP were spherical in shape while some indicate possible sedimentation after some time. It was clearly observed that the particle was a single crystalline with an inter-planar spacing of 0.236 ± 0.006 nm. The SAED patterns of electrons associated a polycrystalline structure indicating its random orientation. They further investigated for the NPs application to nanophotonics and spin-orbit interactions. On measuring Stoke's parameters at 2 different position their interaction was quite similar. Further measuring of the Ellipse orientation (ψ) and ellipticity angle (χ)confirmed the presence of polarization modulation obtained upon the scattering of the transverse magnetic polarized beam by Ag NPs.[9]

Extracellular synthesis of Silver nanoparticles

Another attempt of synthesis of silver nanoparticles was made by Narayanan et al in 2011. They experimented on the biochemical approach of the silver NPs of the *Coleus amboinicus*. Extract preparation was done by taking 20g in mL of DDW for about 03 min. Different parts of the above prepared extract were added to 10mL of 10^{-3}M aqueous solution of $AgNO_3$. Different Silver colloids were synthesized with an immediate colour change to yellowish brown and bioreduction of the silver ions which existed for a longer time was monitored by periodic sampling and analysing the UV-Vis spectra. This solution of the nanoparticles was diluted with deionized water 20 times to avoid errors that could be produced by the high optical density of the solution. An increase in the concentration of the leaf extract decreased the reaction time. The researchers then characterized the NPs by analysing UV-Vis spectra, powder XRD analysis, TEM and FTIR. The optical thickness was used as a measure of the efficiency of particle formation. UV opted for analysis and the 03 different concentrations showed decreasing order of wavelength 457 nm for the smallest concentration and 437nm for the largest concentrations. On increasing concentrations of the leaf extract, they observed Blue shift. XRD analysis and Braggs reflection resulted in the reference of the unit cell

to be FCC as they observed intense peaks at (111), (200), (220), (311) with a lattice parameter: a = 4.079 A˚. The size of the nanoparticles was quite fairly in agreement with the TEM analysis which was determined to be about 25.83±0.78nm. The weaker signals are supposed to rise from X-Ray emissions from proteins or enzymes which are bound to the NPs or in their vicinity. FTIR analysis was carried out to identify all the possible reducing and stabilizing biomolecules. The stronger bands corresponded to C-N vibration of aromatic amines, C=O of amide I and –NH bond of amide II. The weaker bands characterised the C-OH of secondary alcohols. All these are used as reducing and capping agents of silver nanocrystals. HR-TEM analysis was done to analyse the nanostructure of the various particles, the various concentrations of the NPs showed different types of structure. The one with the smallest concentration revealed the formation of anisotropic nanostructures of triangles, truncated triangles, decahedral and little spherical morphologies in the range of 2.6– 79.8 nm in size with an average of 35.8 nm. Whereas the middle concentration showed little anisotropic and more spherical structures truncated triangles and decahedral in the range of 4.9– 55 nm in size with an average size of 30.6 nm. In the colloid with the highest concentration there were signs of isotropic spherical structure predominantly in the range of 4.3 to 40.4 nm size with an average size of 17.6 nm. Finally they concluded that the biosynthesized approach of the silver NPs of *C. amboinicus* was a simple and benign method and that the silver ions of increasing concentration reduced from anisotropic to isotropic structures.[10]

Biosynthesis of Silver and Silver-Gold alloy nanoparticles

Vidya Vilas et al in 2016 attempted the synthesis of silver nanoparticles of *Coleus aromaticus* along with evaluating the antibacterial antiradical properties. For this they steam distilled 300g of fresh leaves to obtain the essential oils using a Clevenger apparatus. Further, 2mL of Stone's solution with 13mL ethanol and 10mL water was used to prepare the diluted oil which acts as a reductant and surfactant. For the synthesis of the Ag NP 40mL 2.49 x 10^{-4} M HAuCl4 solution, 11.5 mL of the diluted oil is added slowly with vigorous stirring at 373 K, which is maintained at a pH of 7. Rapid formation of the NP is seen by the appearance of Violet colour. The colour of the colloid may change to red by increasing the quantity of Haucl4. The synthesis of bimetallic colour is indicated by the colour change from colourless to light violet to dark yellow. Procedure is repeated to obtain various colloids by varying the Au:Ag ratios and thus the colour varying from golden yellow to dark red. Characterization of the mono and bi metallic NPs were done by UV analysis TEM, XRD, FTIR, XPERT and EDS. Other than these, the group performed Antibacterial activity testing, Catalytic reduction, antioxidant activity oxygen scavenging OH radical scavenging and NO scavenging activities. UV analysis of the synthesized NPs constituted of the preliminary techniques for characterization considering the high sensitivity, morphology, refractive index etc. The metal NPs exhibit excitation in the visible region from surface plasmon vibrations, giving out an intense narrow and symmetrical band in the range of 520 -540 nm for gold colloids. Variation in the peak intensity corresponds to the enhanced formation of the NPs by increasing the concentration of the bioreductant. Single plasmon band is a characteristic of the Bimetallic NPs which indicates their homogeneity with the volume. On the contrary, 1:1 ration of the Ag:Au showcased double plasmon bands. To better understand the morphology of the NPs TEM micrographs were analysed. They showed irregular anisotropic AuNPs with 15mL of the reductant. When the concentration was increased spherical shape with average size of 28nm was obtained. The Bimetallic NPs of varying ratios dsiplayed a decremental size range of 17nm as compared to the mono metallic ones which showed 14nm and 20nm. The spacing between atoms was also found for the various concentrations was found. The elemental analysis and quality of NPs was ascertained by the energy dispersive X-ray spectral analysis for some concentrations of the colloidal solution of the NPs. Signals found at 2.9 and 3.1 keV correspond to the Lα and Lβ lines of Ag. K core levels was determined by less intense signals at 22 and 25 keV. While for Au M and L signals were obtained at 1.7 and 2.2keV, 11.5 keV and 13.1 keV. In addition to the two main metals used in the biosynthesis the elemental analyses disclosed the presence of carbon (0.25keV), oxygen (0.52 keV) and Copper (0.9, 8 and 8.9 keV). Structural studies were studied by XRD and FTIR processes. XRD showed braid intense and sharp peaks for the Au/Ag alloy at 38.9°, 44.8°, 65.2°, 78.0°, 82.1° corresponding to the FCC face centred cubic crystalline structure. FTIR analysis of the *C.aromaticus* oil and photosynthsised NPs unveiled the molecules which are involved in the reduction as well as stabilization. Terpeniods were present in the alloys which play a major role in the reduction. Asymmetric C=C stretching vibrations is absent in the alloy, indicating the active participation of the aromatic rings in reduction. Ortho substituted C-H bending vibration was also seen in the AuNPs. Also the appearance of moderately intense band at 1724 cm^{-1}in alloy indicates the oxidation of terpenes to aldehydic compounds during reduction of the metal ions. Catalytic degradation was done on aromatic Nitro compounds. Isomers of nitrophenol were singled in alkaline medium where they exhibited broad peaks due to formation of the corresponding nitro phenolate ions. This is otherwise a slow reaction which completed in a span of minutes when the synthesized NPs were added. Among the isomers of nitro phenol, the alloys were effective in degrading Nitrophenol at a rate constant of 0.2088 and 0.3227 min^{-1} and % pollutant removal values of 94.1 % and 94.2 %, respectively. Further they also ascertained the degradation of Azo dyes. The alloys efficiently degraded MO in 06 mins at 95.1 and 97.4 respectively. MR reduction required excess nanocrystals. Fluorescein dye (RB)(EY) degradation was performed to

explore the activity of the alloy NPs. The dyes EY and RB absorbed at 516 and 553 nm respectively on increasing the pH. As the catalytic reduction progressed the intensity of absorption dropped because of the formation of dihydro form from the quinoid on. The rate of reaction decreases on the addition of the NPs. There were evident changes in the %D and K values as well. The researchers attempted to establish the biopotenct of the herbal deduced alloy NPs to exhibit inhibitory effect on *S. aureus* (gram positive) and *E.coli* (gram negative). The alloy NPs displayed appreciable decline in the growth of bacteria in the inhibition zone. The inhibition zone diameter for *E.coli* was around 2.8 and for *S.aureus* it was found to be 1.8. The main cause for choosing the study of the NPs antioxidant property was because of presence of Transition elements in the NPs. O2 NO and OH which are some of the most toxic radicals were chosen to portray the antiradical activity. In the presence of the alloys the chromophore showed decreased absorbance at 565nm. They finally concluded by stressing on the approach of using alloys for the NPs and their applications in the chemical and environmental applications.[11]

Caesium nanoparticles

K. Ramya et al in 2022 thus researched about the Caesium carbonate nanoparticles using *C. amboinicus*. For this they used 05gm of dried and powdered leaf sample then subjecting it to 32 cycles of soxhlet extraction using distilled water. Extract then concentrated using rotatory evaporator and the percentage yield was calculated. Caesium carbonate was prepared mixing 0.1M and 0.1M concentrations of Caesium Chloride in a combination of 1:1 proportion. For preparation of the nanoparticles, 25mL of the leaf extract was added and stirred with a magnetic stirrer and Caesium mixture solution was added drop wise till colour change. This was then covered in Aluminium foil, incubated for 24hrs at room temperature (27°C). The accumulated precipitate was further dried in a hot air oven. The researchers then characterized the vacuum dried powder using UV- Vis, FTIR, SEM and XRD techniques. Absorbance of Caesium carbonate in the sample was between 200-800nm. The peaks at 290nm and490nm confirmed the presence of Caesium carbonate nanoparticles. The technical analytical method of FTIR showed the presence of many organic functional groups. The absorption band detected the presence of phenol(attributed to -OH stretching), Carboxylic acid and Terpenes.The SEM analysis conducted showed irregular hexagonal shape of Caesium Carbonate structure. It also gave an idea about the range of particle size which was approximated at 75-110nm and also investigated the morphology of the nanoparticles. The XRD analysis characterized the crystalline material of the synthesized nanoparticles. There were about 09 prominent peaks observed to the following crystal coordinates such as (001), (011), (111), (012), (112), (200), (113), (202) and (220). This confirmed that the thus formed Caesium Carbonate nanoparticles had a multi-planar hexagonal crystalline structure. Along with this K. Ramya et.Al also studied the Bioactivity of biosynthesized caesium carbonate nanoparticles testing its Total Antioxidant, DPPH Radical Scavenging Assay, BSA Inhibition Assay, Protease Inhibitor Assay and Antibacterial Assay. The assay of antioxidant was evaluated using Total Antioxidant Assay method. Standard used was ascorbic acid and the Cs_2CO_3 showed valuable antioxidant property. The unknown sample concentration was found to be 90.86 µg/ml. DPPH radical scavenging assay of the biosynthesized nanoparticles was analysed for the substantial antioxidant activity. They showed efficient antioxidant activity when ascorbic acid was used as the standard. Anti-inflammatory activity was determined by the BSA Inhibitory Assay using the percentage of protein denaturation. It was further thus observed that on increasing the concentration the percentage of inhibition also increased. Further they performed the Protease Inhibitory Assay for protein denaturation. The synthesized nanoparticles gave considerable effect with increase in concentration. For deducing the antibacterial activity well diffusion method. They investigated on both Gram Positive (*E.coli*) and Gram Negative (*S. aureus*) with different concentrations. It was observed that at concentration of 60mg/mL the nanoparticles showed highest zone of inhibition in both *E.coli* (20mm) and *S. aureus* (22mm) and minimum at a concentration at 30mg/mL. They finally concluded that green synthesized nanoparticles of *C. amboinicus* with Caesium Carbonate showed high bioactivity and hence can be targeted to personalize bio therapeutics.[12]

Copper nanoparticles

Srividya Parthasarathy et al. in the year 2020 experimented to synthesize nanoparticles using the leaves of *P. amboinicus*. Extract was prepared using 100mL of distilled water and boiling on a hot plate. Then leaves were strained using a filter cloth, cooled at room temperature and stored in the deep freezer. The extract has reducing properties which aided the reduction of aq. Copper sulphate into copper nanoparticles. 02mL of the leaf extract was added in 10mL copper sulphate solution by the help of a magnetic stirrer. After incubating overnight the solution changed colour from light to dark green. It was further centrifuged at 12000 rpm for a time of 10-15 min to obtain pellets of Copper Nanoparticles which were stored at 4°C for further characterization and analysis. They proposed that the important factor of metal nanoparticles was their optical properties changed due to the morphological characteristics of the nanoparticles. For the characterization they performed UV-Vis spectroscopy, XRD technique and Zeta potential. They checked the peak of UV after 24 hrs, whose absorbance was between the ranges of 230-270nm. They also explained how higher conversion of copper sulphate to copper nanoparticles gave higher absorbance corresponding to its high concentration. The analytical method of XRD for determining the size and crystalline nature of the particles. The nanoparticles reflected high degree of crystallinity was by the intensity

and sharpness of the peaks at 34.96°, 41.50°, 58.37°, 69.34°and 75.57°. Grain size of Copper nanoparticles was estimated at 21.47nm. Planes values was observed at (111), (200), (220), (311), (222). As the diffraction peaks were defined and indexed using Face-Centred cubic cell with average lattice parameter to be 4.4195 Å. The Zeta potential was determined. The Z- average was obtained as 5.3nm using DLS. Charge obtained using this Zeta analysis was -25.2mV. The particles that had negative charge had stronger force of repulsion indicating stability and quality. They concluded that the Copper nanoparticles of *P. amboinicus* was both a reducer and stabilizer and for it to be one of the best plants for production of copper nanoparticles by the eco-friendly green synthesis method.

Second attempt of synthesis of copper nanoparticles was made by K.Velsankar et al in 2020. They biosynthesised copper nanoparticles of *Plectranthus amboinicus* using its leaf extract. About 10g of the leaf extract was made to mingle with 75 mL of deionised water and then heated to 70°C for about 45 mins. Further filtration was done using Whatman no 1 filter paper to obtain a clear, residual- free solution of the leaf extract. 20mL of the extract was then added to 0.1 M of Cupric Nitrate (Cu(NO3)2) prepared using 80 mL deionised water, warmed at 70 °C with repeated stirring for about 03-04 hours. Colour change was detected from blue to bluish green to further dark green. The solution was centrifugated, precipitated, dehydrated, calcinated and grained to obtain CuO solid powdered NPs. Characterization of the hence synthsised CuO NPs of *P. amboinicus* was done using XRD, FTIR, UV, Photolumiscence, Particle size analyzer and Morphological, structural and mapping analyses. Along with this their antibacterial, antioxidant, anti-inflammatory, antidiabetic and antilarvicidal was also analysed. XRD manifestation of the NPs was done with the spotting of the peaks at 32.22°, 35.42°, 38.64°, 48.60°, 53.20°, 56.67°, 58.02°, 61.32°, 66.10°, 68.05°, 71.96° and 74.80°. This pattern stained denoted the formation of Monoclinic Crystalline nature of the CuO NPs of *P amboinicus.* The mean size was obtained by the Scherrer's formula which was in the range of 20-35 nm, determined lattice strain at 0.0048 and calculated dislocation density at 1.65 × 10 15 m-2. The FTIR consisted of bands which were in charge of reduction via biological capping and also metal-oxygen bonding. The major bands correlated to OH hydroxyl group, Amide I group of proteins/ enzymes, CN amine stretching and Carboxylic acid stretching. There were also strong intense peaks due to the existence of Cu-O bond. UV analysis showed an SPER band at 398nm which may be based on the small size of the NPs. This caused inter and core electrons transition of Cu metal in the NPs. SPR bandgap was determined at 3.11eV illustrating a blue shift because of quantum confinement. Photolumiscence of the NPs was conferred along with the optical property with the emission peaks at 361nm, 413nm, 438nm, 491nm and 529nm. All the peaks ascribed various processes of the recombination, some defects and oxidation states of copper etc. The particle size analyser was determined by the dynamic light scattering which was in the range of 05-40nm. The polydispersity index reached 0.288, this indicated the ability of the NPs to deliver drugs in tissue and other applications. The structure, shape and size were confirmed with HRTEM micrographs displaying circular, spherical and rectangular monoclinic structured. The size range was majorly under 05-30 nm. The nature of the NPs emerged was a well-defined and ordered arrangement of lattice planes by the emergence of fringes. The antimicrobial activity of the NPS was tested using *Escherichia coli, Klebsiella pneumonia, Pseudomonas aeruginosa, Staphylococcus aureus, Streptococcus pyogenes, Bacillus subtilis, Aspergillus favus, Aspergillus niger, Candida albicans and Candida tropicalis.* NPs were taken in different concentrations and chloramphenicol was taken as standard. Higher concentrations that were applied showed a higher inhibition value. Antioxidant activity was analysed by DPPH method which provided the activity of free radicals. The inhibition percentages of CuO nanoparticles were 28%, 49%, 79% and 94%. The IC50 value received for CuO nanoparticles was at 40.10 µg/mL taking ascorbic acid as standard. Anti-inflammatory activity was compared to Diclofenac sodium with the inhibition percentage found to be 26%, 46%, 65%, 83% and 92%. The IC50 value reached for CuO nanoparticles at 243 µg/mL, this stated the efective potent nature of the anti-infammatory activity of synthesized CuO nanoparticles. Anti-diabetic activity was manifested with acarbose as standard. The inhibition percentage received for formed CuO nanoparticles was at 17%, 27%, 46%, 76%, 94% and IC50 value achieved for formed CuO nanoparticles was at 317µg/mL. These results proved that the anti-diabetic activity of formed CuO nanoparticles was similar to insulin secretion than standard chosen. Antilarvicidal acitivity was checked using larvae of *Anopheles subpticus* mosquito. CuO NP caused the inhibition by accumulation and growth in the alimentary canal and siphon region in the respiratory canal. Thus, the mosquito die by suffocation. Moreover ions and small size of the NPs are quite effectively toxic to the mosquito larvae. The concluded by describing the biogenic use of CuO NPs of *P. amboinicus* and their various characterization and applications.[13]

Green synthesis of zinc nanoparticles

Peng Wang et al in 2020 attempted the bio-inspired synthesis of Zinc nanoparticles of the leaf extract of *C.amboinicus* along with investigating its application in antimicrobial treatment for burn wound infections. For the extract preparation they had taken 20g of finely powdered sundried leaves which was boiled in 100mL DDW for 40mins at 90°C. In order to obtain a clear solution of the extract the above mixture was cooled and filtered using Cellulose Nitrate membrane. Moreover for the NPs synthesis 50mL of the above prepared extract was boiled at 60°C-80°C using a stirrer heater. To it, 05g of Zinc Nitrate was added until they received a deep yellow paste. This was then shifted to a crucible for

heating in a furnace till it resulted in light white coloured powder. This powder was utilized for further characterization and biological studies. They tested the Zinc NPs for UV, XRD patterns, TEM and FTIR. UV spectroscopy was analysed where upon they observed peaks at 396nm, 418nm (may be because of Zn vacancy), emission at 450nm corresponding to O_2 vacancy and similar emissions at 466nm, 481nm and 492nm corresponding to the vacancy and interstitials of Zn and O_2. On obtaining results of XRD patterns analysis they also confirmed the Wurtzite structure of the synthesized ZnO NPs. Furthermore, they observed no impurities in the crystalline form indicating its purity. Its crystalline preferred orientation was seen due to its anisotropic growth. On calculating the size of the NPs by the Debye-Scherrer equation, the results were found to be 15nm. The fabricated images of ZnO NPs was viewed at various magnifications under the TEM. They observed that the particles were polydispersed with a size range of 15-20 nm the FTIR analysis detected the presence of aromatic C-H in typical mono substituted benzene ring, 1, 4 di-substituted benzene ring and 1, 2, 3 tri substituted ring of benzene, another band for C–N bond present in amine functional group. On the other hand the absorption bands confirmed the existence of aromatic aldehyde, of C≡C bond and also OH which had a broad and intense band. Along with this, the vibrations which corresponded to the aromatic ring also proved that phyto extract biomolecules could enhance the ZnO NPs stabilization via capping in the aqueous medium. For antimicrobial testing they took 05 strains of various pathogenic microbes and used the Kirby-Bauer method for testing. The low concentrations of ZnO NPs exhibited moderate activity for both types of bacteria; but when DMSO was utilized as a solvent no antibacterial effect was seen. But it was observed that the gram positive ones were more resistant than the negative ones to the treatment of ZnO NPs. One of the researchers investigated the NPs on Mesophilic and Halophilic microbial species and further demonstrated that *B.subtilis* is less sensitive then *Enterobacteria*. They concluded the antimicrobial study by reporting that the existence of peptidoglycan thick layer in the cell wall of Gram-Positive bacteria is responsible for its resistance. They majorly investigated on the burn and wound healing properties of the biosynthesized ZnO NPs in the Rat model. On day 07, 14 and 28 the groups were checked on the inflammation, hyperaemia and also redness. On comparing with the untreated group and SSD groups, fast wound contraction was inferred in the rats treated with ZnO NPs. After the 28 days of wound formation, control and the SSD groups showed mild redness, with no indication of inflammation, hyperaemia and redness was observed in the group administrated with ZnO NPs. It was thus concluded that the ZnO NPs of *C. amboinicus* were synthesized and characterized. Along with them showing antimicrobial action, they also proved to have satisfactory wound and burn healing properties, suggesting them to be a good dressing material for wound healing.[14]

S. Vijayakumar et al in 2014 attempted the green biosynthseis of *Pelctranthus amboinicus* using Zn NP. 30g of air dried leaves were used for the preparation of the extract for NPs synthesis. These were then boiled with 250 mL Sterile DW at 100 °C, using Whatmann filter paper no.1. This leaf extract was then added to 0.05mM Zinc Nitrate solution under magnetic stirrer. After stirring for about 06 hours at a high temperature, it was allowed to cool down and the supernatant was later discarded. A pale white solid that had been obtained was later washed with DW at 4500 rpm for 15 mins. This is later dried for 07-08 h at 80 °C. Further characterization of the synthesized NPs was done via UV, TEM, XRD and FTIR. Microbiological assay was also done by 03 different methods agar diffusion assay, biofilm assay and in vitro biofilm inhibition assay. UV-VIS spectroscopy analysis of the biosynthesized NP was done for about 06 hours at 150 °C. They exhibited strong UV absorption in the range of 360-370nm due to its SPR attaining a plateau above 3.3eV. Furthermore, XRD and TEM was performed. The XRD patterns of the NPs revealed attributes of a crystalline nature because of the strong diffraction peaks at various degrees of 2θ. These peaks corresponded to (100), (002), (101), (102), (110), (103), (200), (112) and (201) crystal planes which signified the Hexagonal wurtzite structure of the NPs. TEM analysis revealed that the NPs powders which were agglomerated particles, spherical and also hexagonal with an average size range of 20-50 nm. They also analysed the NPs for FTIR to identify the possible biomolecules along with the characterization of the interaction sites of *P.amboinicus* extract and Zn NPs. Biomolecules like primary and secondary amines, O–H stretching of alcohols, C–H stretching of alkanes, bending vibrations of N-H in secondary amines of proteins. Carbonyl and carboxylic (C = O) stretching bands of peptide linkages (stretching of amides) along with C-C and C-N stretching. *P. amboinicus* extract considered as the capping ligands which give stability to the ZnO NPs. S. Vijayakumar et al in their synthesized NP analysed for the antibacterial activity of the NPs with a range of varying concentration from 02 -10 µg/ml after 24 hours of incubation. They proposed that the inhibition of bacterial growth by ZnO nanoparticles could be attributed to damage of the bacterial cell membrane and extrusion of the cytoplasmic contents thereby resulting in the death of the bacterium. The antibiofilm activity of the NPs of the extract was studied by the researchers by MRSA ATCC 33591 by biofilm formation using a crystal violet staining MTP method. The disruption of biofilm structure after treatment with the nanoparticulates was evident from confocal microscopy. This was seen at a concentration of (10 µg/mL), which was assessed and visualized under confocal laser scanning microscopy (CLSM). The larvicidal activity for the synthesized particles were also studied against different larvae of *A. stephensi*, *C. quinquefasciatu*s and C. *tritaeniorhynchus*. For *A. stephensi* and *C. quinquefasciatus* lower concentration (8 mg/L) of the NPs were shown to give 100% mortality and *C.*

tritaeniorhynchus required a higher concentration for a 100% mortality (14 mg/L). This then associated the use of the biosynthesized as a vector control as it could reduce the mosquito populations at the larval stage. Thus, they concluded that the NPs they synthesized could be used as mosquito larvicidal along with them being antibacterial and antibiofilm drugs for biomedical purposes.[15]

Yuhong Zheng et al in 2019 attempted the biosynthesis of *Pelctranthus amboinicus* with zinc oxide. Here, 05g of plant leaves were boiled with 30mL of DW for 15 mins at 100°C, filtered using Whatman no. 01 filter paper. Aqueous 0.1 M of zinc nitrate solution was prepared. To this 10mL of the extract was added and kept at 80°C for approximately 04 hours. The obtained pale white precipitate was washed with ethanol and water. Further characterization was done by then using SEM, XRD and FTIR. SEM characterization helped in the analysis of the study of the morphology of biosynthesized and chemical synthesis of the ZnO NPs. The biosynthesized ones were in rod shape with slight aggregation with particle size average of 88nm and a range of 50-180 nm; while the chemical ones were spherical in nature in the size of 74 nm. EDX analysed the elemental information of the both types of synthesis of the NPs. Using signal counts the strength of Zinc and Oxygen was found to be 75% and 23% respectively which inferred that the biosynthetic method resulted in a good quality NOs as compared to the chemical method. XRD analysis indicated that both of the methods yielded in pure and crystalline particles. The planes of the patterns indexed at (100), (002), (101), (102), (110), (103), (112) and (201). This planes showed no signs of impurity, proposing methods for good quality Zn NPs. The structure was around to be Hexagonal Wurtzite in nature. FTIR absorbance ranged in the range of 700- 2000cm^{-1}. In the range they found bands associated with C-O belonging to polysaccharides polyols, C-N Vibrations of nitroso group. The biosynthesized ZnO NPs were then used for modification of GCE surface and its electrocatalytic detection performance towards NOX. With the modified GCE displays the Zn NPs were seen to have a wide detection linear range of 1-50 IM with a relative low detection range limit for NOX sensing.[16]

Green biosynthesis of SnO_2 nanopticles

L.FU et al in 2015 attempted green biosynthesis of sno2 nanoparticles by *Plectranthus amboinicus* leaf extract along with their photocatalytic activity toward rhodamine b degradation. Then, 5g of *P.amboinicus* leaves were washed with water and extract was obtained on sonication for 1 hour following filtration which was done using Whatman no 1 filter paper. Further for the synthesis of SnO_2 NPs, zinc nitrate solution (0.5 M) was added to 30mL water. To this solution the above prepared extract (20ml) along with 0.5ml H_2SO_4 was added. This was then autoclaved, centrifuged and calcined to result SnO_2. The thus synthesized SnO_2 NPs were further characterized by analytical methods like FESEM, XRD and UV Vis spectrophotometer. The SEM images were observed at different magnifications showing a cluster structure. The individual particle size could not be visually measured due to aggregation. The average size of biosynthesized SnO_2 NPs 63nm was analysed by particle size analyser. The XRD EDX spectrum of the biosynthesized SnO_2 NPs had confirmed the presence of tin and oxygen along with no impurities indicating the reliance of the method used. The crystal structure was determined using well defined diffraction peaks observed at 26.75°, 37.88°, 39.35°, 51.95°, 54.50°, 57.93°, 62.09°, 64.95°, 66.08°, 69.32°, 71.70° and 79.13° C. Using UV-Vis Spectroscopy the light absorbance and disuse reflectance was observed. It was clearly observed that the biosynthesized SnO_2 NPs exhibit a higher absorbance than commercial SnO_2. The photo degradation effects were investigated by using the Langmuir and Hinshelwood models of Rhodamine B and compared to commercial SnO_2 NPs with respect to time. The decreasing concentration with time was attributed to the cleavage in the aromatic ring. The biosynthesized NPs displayed quite a high performance of more than 95% in after 120min light illumination. They finally concluded that *P.amboinicus* was achieved by one- pot hydrothermal approach and these showed a superior photocatalytic performance towards dye degradation.[17]

Phytosynthesis of gold nanoparticles

K.B.Narayanan et al 2010 attempted the biosynthesis of Gold nanoparticles with *Coleus amboinicus*. For this 20 g of leaves were boiled with 100mL DDW, filtered and stored at4 °C. 02mL of this extract was kept in the dark at 30°C on addition to 10 ml of 10^{-3} M $HAuCl_4$ aqueous solution. The bioreduction was monitored by specific sampling of the aliquots of $AuCl_4^-$ ions. The colour change after 01 hour from pale yellow to pink ruby indicated the completion of the reaction and the formation of gold nanoparticles. Further characterization was done in triplets for UV-Vis spectra followed by XRD, SEM, TEM, EDAX and FT-IR. For UV-Vis spectra the major band of the Gold SPR spectra was centred at around 536nm. Following this, they performed XRD, resulting in intense peaks corresponding to the FCC structure of the biosynthesized NP of Gold. Mean size calculated using the Debye–Scherrer's equation for the (111) peak was observed at about 23.7± 0.72 nm for the NPs. They performed SEM to determine the size range which was observed at around 50-80nm at a magnification of 23 times. EDAX spot profiles showed weak signals for the Carbons atoms while the Gold atoms gave out stronger signals. They also signalled the possibility that the weaker signals might have been risen from the marcomolecules (proteins/enzymes) which were bound to the NPs or were in its vicinity which could have emitted X-Ray. FT-IR analysis identified the possible bioreducing molecules in the leaf extract. Various functional bands gave out their corresponding spectra which included C-N stretching of aromatic amines. Some vibrations corresponded to C=O stretching of amide I band, –NH stretching in amide (II) and characteristic

vibration of C–OH stretching of secondary alcohols. Some of the weaker bands corresponded to assymetric stretching of C-H functional groups. FT–IR spectrum done here confirmed the presence of aromatic amine, amide (II) groups and secondary alcohols as capping and reducing agents of gold nanoparticles. On performing HR-TEM analysis for the Gold NPs they observed the formation of stable morphologies like spherical, triangle, truncated triangle, hexagonal and decahedral which ranged from 4.6 to 55.1 nm in size at a 50X magnification. The spherical NPs produced at the start were quite stable in contrast to the crystals formed in latter stage of the synthesis. They stressed on the various shapes of the Gold NPs, the stage of their synthesis and on the reason behind their structure. They concluded the paper by briefly explaining their uses and the role of its functional groups towards the synthesis of gold NPs[18].

Synthesis and characterization of Titanium nanoparticles

Mathiyazhagan Narayanan et al in 2021 researched on the biosynthesis of *Coleus aromaticus* with Titanium along with experimenting on its antibacterial, larvicidal, and anticancer potential. About 10g of the leaf sample was crushed and added to distilled water 100mL. Hot extraction process was followed where homogenisation of the sample was carried out at 60°C for about 10 min. This was then filtered the sample using Whatman no.1 and the extract was produced. For the Nanoparticle fabrication, 40 mL of the aqueous extract was added to 160mL of 01mM TiO_2 with constant stirring for 24 hrs. Upon the completion of 24hrs a notable colour change in the reaction mixture is observed confirming the bioreduction process of extract with TiO_2. Characterization process was done with the help of UV, XRD, EDX, FTIR and TEM. The phytochemical constituents of the extract had the potential to reduce and form NPs with TiO_2. With UV Vis spectrophotometer the highest peak was observed at 332nm. Colour change was seen from light green to dark brownish green indicating the completion of synthesis of the TiO_2 NPs. XRD analysis was confirmed with various diffraction angles. Peaks revealed the existence of Tetragonal structure with planes at (111), (200), (220), and (311) respectively. Multiple Functional groups were disclosed during the FTIR analysis. The acquired peaks corresponded to phenols, carboxylic acid, alkanes, unsaturated esters, primary amines, aromatics, aliphatic amines, alkynes, and metal oxygen. The prominent peak of the NPs was reported of the O-H stretching of phenols indicated its high volume. EDX analysis showed that the signal developed by titanium in the NPs was with an atomic percentage of 52.64%. The remaining percentage was occupied with Carbon, Copper and Oxygen. This suggested that the obtained particles was partially purified. The size and shape of the NPs were analysed under TEM studies with shape of hexagonal structure with reasonable disparity and size range of 12-33 nm average being 16.5nm. The TEM was seen because of the nature of reducing agents and their exposure time. The larvicidal potential was carried out for various concentrations of the nanoparticles of *Coleus aromaticus*. They showed significant action against I-IVth instar larvae of *Ae. aegypti* mosquitoes. LC 50 value on 24 hours were 15.222, 32.621, 43.536, and 52.336 µg L^{-1}, respectively and LC90 values were recorded as 132.763, 130.925, 128.394, and 178.314 µg L^{-1}, respectively. IVth instar showing the highest mortality while III instar being the least. These results indicated that the TiO_2 NPs of *C.aromaticus* could be considered as a suitable agent for *Ae. aegypti* mosquito management. Antibacterial competence of *C. aromaticus* TiO_2 NP was checked using pathogens like *Shigella boydii, Vibrio cholerae,Bacillus cereus, Aeromonas hydrophila, Enterococcus faecalis, and Bacillus megaterium*. The results that were acquired with standard, Chloramphenicol. Inhibition zone of 3mgL-1 was found to be *E. fecalis* (33 mm) and *S. boydii* (30 mm) as contrasted to other pathogens which was comparable to the standard. The potential of the NPs was directly related to their crystalline structure and capping elements. Cytotoxic assay was accomplished in HeLa cell line to assess the anticancer proficiency of the synthesized NPs. various concentrations of the NPs were incubated with HeLa cell line for 24 h. The percentage of Hela cell line viability decreased with the increasing concentration. 92.37% inhibition of the cell was observed at the highest concentration of 200 µg mL^{-1}. They concluded that this synthesis was eco-friendly and a one-step process along with discussing the various activities and characterization properties of the thus green synthesized TiO_2 nanoparticles of *Coleus aromaticus.*[19]

CONCLUSION

Metal and metal oxide nanoparticles have a very wide range of scientifically proven uses in various fields. To overcome the environmental challenges posed by chemical methods (where hazardous chemicals are used) and requirement of big, costlier machineries in physical method of fabrication of nanoparticles, an eco-friendly approach has been developed involving the use of plant extracts for green synthesis of various nanoparticles. *Coleus amboinicus* (Lamiaceae) leaves contain numerous phytochemicals, which are made available for the reduction of donor compounds to respective nanoparticles by extraction using appropriate solvent. Based on this review, it can be concluded that due to the presence of few non-polar phytoconstituents, *C. amboinicus* leaf extracts can be used for green synthesis of nanoparticles of different metals and metal oxides having a wide range of applications.

ACKNOWLEDGEMENT

We, the authors of this review article are thankful to Managerial Board, Alard Charitable Trust's Alard College of Pharmacy, Marunje for providing internet and library facilities for carrying out literature survey.

REFERENCE

1. Hasan, S., A review on nanoparticles: their synthesis and types. *Res. J. Recent Sci.*, 2015; *2277*: 2502.
2. Mohanraj, V.J. and Chen, Y., Nanoparticles-a review. *Tropical journal of pharmaceutical research*, 2006; *5*(1): 561-573.
3. Khandel, P., Yadaw, R.K., Soni, D.K., Kanwar, L. and Shahi, S.K., Biogenesis of metal nanoparticles and their pharmacological applications: present status and application prospects. *Journal of Nanostructure in Chemistry*, 2018; *8*(3): 217-254.
4. Wadikar, D.D. and Patki, P.E., Coleus aromaticus: a therapeutic herb with multiple potentials. *Journal of food science and technology*, 2016; *53*(7): 2895-2901.
5. Punet Kumar, S. and Kumar, N., Plectranthus amboinicus: a review on its pharmacological and pharmacognostical studies. *American Journal of Physiology*, 2020; *10*(2): 55-62.
6. Mallikarjuna, K., Reddy, L.V., Al-Rasheed, S., Mohammed, A., Gedi, S. and Kim, W.K., Green synthesis of reduced graphene oxide-supported palladium nanoparticles by Coleus amboinicus and its enhanced catalytic efficiency and antibacterial activity. *Crystals*, 2021; *11*(2): 134.
7. Bathula, C., Subalakshmi, K., Kumar, A., Yadav, H., Ramesh, S., Shinde, S., Shrestha, N.K., Mallikarjuna, K. and Kim, H., Ultrasonically driven green synthesis of palladium nanoparticles by Coleus amboinicus for catalytic reduction and Suzuki-Miyaura reaction. *Colloids and Surfaces B: Biointerfaces*, 2020; *192*: 111026.
8. Vanaja, M. and Annadurai, G., Coleus aromaticus leaf extract mediated synthesis of silver nanoparticles and its bactericidal activity. *Applied nanoscience*, 2013; *3*(3): 217-223.
9. Prajapati, C., Jolly, A. and Ravulapalli, S., Bio inspired synthesis of silver nanoparticles and its applications to spin–orbit interactions of light. *Nano Express*, 2020; *1*(3): 030031.
10. Narayanan, K.B. and Sakthivel, N., Extracellular synthesis of silver nanoparticles using the leaf extract of Coleus amboinicus Lour. *Materials Research Bulletin*, 2011; *46*(10): 1708-1713
11. Vilas, V., Philip, D. and Mathew, J., Biosynthesis of Au and Au/Ag alloy nanoparticles using Coleus aromaticus essential oil and evaluation of their catalytic, antibacterial and antiradical activities. *Journal of Molecular Liquids*, 2016; *221*: 179-189.
12. Ramya, K., Ramalingam, R.J., Nethra, V., Zuha, S.S., Yuvaraj, D., Al-Lohedan, H., Arokiyaraj, S. and Alqahtani, H.M., 2022. Green synthesis, characterization and bioactivity evaluation of Caesium carbonate nanoparticle using Coleus amboinicus.
13. Velsankar, K., Vinothini, V., Sudhahar, S., Kumar, M.K. and Mohandoss, S., Green Synthesis of CuO nanoparticles via Plectranthus amboinicus leaves extract with its characterization on structural, morphological, and biological properties. *Applied Nanoscience*, 2020; *10*(10): 3953-3971.
14. Wang, P., Jiang, L. and Han, R., Biosynthesis of zinc oxide nanoparticles and their application for antimicrobial treatment of burn wound infections. *Materials Research Express*, 2020; *7*(9): 095010.
15. Vijayakumar, S., Vinoj, G., Malaikozhundan, B., Shanthi, S. and Vaseeharan, B., Plectranthus amboinicus leaf extract mediated synthesis of zinc oxide nanoparticles and its control of methicillin resistant Staphylococcus aureus biofilm and blood sucking mosquito larvae. *Spectrochimica Acta Part A: Molecular and Biomolecular Spectroscopy*, 2015; *137*: 886-891.
16. Zheng, Y., Huang, Y., Shi, H. and Fu, L., Green biosynthesis of ZnO nanoparticles by plectranthus amboinicus leaf extract and their application for electrochemical determination of norfloxacin. *Inorganic and Nano-Metal Chemistry*, 2019; *49*(9): 277-282.
17. Fu, L., Zheng, Y., Ren, Q., Wang, A. and Deng, B., Green biosynthesis of SnO2 nanoparticles by amboinicus leaf extract their photocatalytic activity toward rhodamine B degradation. *J Ovonic Res.*, 2015; *11*(1): 21-26.
18. Narayanan, K.B. and Sakthivel, N., Phytosynthesis of gold nanoparticles using leaf extract of Coleus amboinicus Lour. *Materials characterization*, 2010; *61*(11): 1232-1238.
19. Narayanan, M., Vigneshwari, P., Natarajan, D., Kandasamy, S., Alsehli, M., Elfasakhany, A. and Pugazhendhi, A., 2021. Synthesis and characterization of TiO2 NPs by aqueous leaf extract of Coleus aromaticus and assess their antibacterial, larvicidal, and anticancer potential. *Environmental Research*, *200*; 111335.